Mining of Mineral Deposits
Volume 16 (2022), Issue 2, 49-54

https://doi.org/10.33271/mining16.02.049

Determining the regional tectonic stress field by remote sensing in the Bou Azzer inlier, Central Anti-Atlas, Morocco

Anas Driouch[1*], Latifa Ouadif[1], Khalid Benjmel[2], Mohamed Bhilisse[3], Said Ilmen[4]

[1] *Mohammed V University, Rabat, Morocco*
[2] *Hassan II University, Casablanca, Morocco*
[3] *Aya Gold & Silver Company, Casablanca, Morocco*
[4] *Ibn Zohr University, Agadir, Morocco*

**Corresponding author: e-mail anasdriouch@research.emi.ac.ma*

Abstract

Purpose. This paper deals with the determination of the regional stress field direction of the Bou Azzer inlier using the remote sensing tool.

Methods. In this study, we use an approach to digital mapping by remote sensing, including the steps of pre-processing and processing of Landsat-8 OLI images. Then, an automatic extraction of lineaments based on directional filtering has been performed. To determine the main directions of major mean fractures, these results have been supplemented and confirmed by an integrated model, including a synthesis of bibliographic works and field studies.

Findings. The directional rosette analysis results show four systems of major directions namely, N0°, N45°, N90° and N135°. The regional stress field in the study area, according to tectonic history, is characterized by a horizontal compression tectonic regime, as indicated by several systems of strike-slip faults with a high tendency to deformation. Thus, the abundance of brittle and ductile microtectonic indicators confirms the direction of the main compressive stress N°30. The direction of the three-dimensional stress field: σ1: N°30, σ2: N°120, σ3: Vertical component.

Originality. The present study allows to determine the regional stress field direction of the Bou Azzer inlier, in particular, in areas affected by complex tectonics of various scales, as well as in hard-to-reach areas.

Practical implications. In mining practice, the study of stability using 2D and 3D geotechnical numerical modeling of underground mine workings is essential. The stress field direction is an important input parameter to develop more realistic decision support models, as well as to ensure the safety of people and materials at the Bou Azzer mine.

Keywords: *Bou Azzer, remote sensing, fractures, engineering geology, stress field, modeling*

1. Introduction

Remote sensing is a technique widely used to study large geographical areas, as well as to perform geological and structural mapping. It is considered a tool for extracting lineaments that correspond to geological fractures or faults. Therefore, the practicality of this study is particularly important in geological exploration, hydrogeology, geotechnical modeling, and mine planning. The term "lineament" was first used in [1] to study the rock topography and is described in [2]-[6]. Many geological surveys used remote sensing data for lineament extraction, including Jbel Saghro in the eastern Anti-Atlas [7], in the Iguerda inlier of the Central Anti-Atlas [8], in the Bas Drâa inlier of the Eastern Anti-Atlas [9], in the Sidi Flah-Bouskour inlier of the Eastern Anti-Atlas [10], and in the Taghdout region of the Central Anti-Atlas [11].

The purpose of this paper is to provide a map of fracturing in the Bou Azzer inlier in order to understand the distribution of fractures and determine the stress field (σ1, σ2, σ3) direction in the study area. Several remote sensing processes have been applied to Landsat-8 Oli image, including pre-processing: radiometric calibration, atmospheric correction, and principal component analysis (PCA) to properly characterize the geological fractures. Conducting validation and interpretation based on bibliographic synthesis and field work, including structural observations and in-situ measurements. Finally, determine the regional stress field direction based on the analysis of the major directional rosettes of the faults.

2. Geological setting

2.1. Lithological context

The Bou Azzer-El Graara inlier (Fig. 1) is located along the major accident of the Anti-Atlas in its central part [12]. In this inlier, the outcrop gives evidence of the oldest formations, which have been subdivided into two major lithological sets according to [13]-[16]. The first group corresponds to the magmato-metamorphic ensemble, more ancient, of Neoproterozoic age, formed by complexes of tecton-

Received: 6 February 2022. Accepted: 22 April 2022. Available online: 30 June 2022

Mining of Mineral Deposits. ISSN 2415-3443 (Online) | ISSN 2415-3435 (Print)

ic scale stacks resulting from the Pan-African collision, formed mainly by orthogneiss, more or less metamorphosed mafic rocks and paragneiss, confined to the Lower Cryogenian age (NP2i). These rocks are intersected by granitoids of the Upper Cryogenian age (NP2s). On the one hand, the second group consists of Neoproterozoic platform deposits occurring on the northern margin of the West African Craton (Tachdamt-Bleïda Group), composed of siltstones, quartzites, sandstones, and basalts confined to the Lower Cryogenian age (NP1-2). On the other hand, the third group corresponds to the Tichibanine-Ben Lgrad volcano-sedimentary series, composed of thin siltstones intersected by granitoids of Taghouni massif of the Lower Cryogenian age [17], [18]. The last group corresponds to the Bou Azzer ophiolitic complex, composed of serpentinized mantle peridotites, cut by a swarm of basic and ultrabasic veins, basic and ultrabasic cumulates, gabbros and microgabbros, spilitized basalts and diabases, as well as a volcano-sedimentary ensemble, confined to the Upper Cryogenian age [17]-[23].

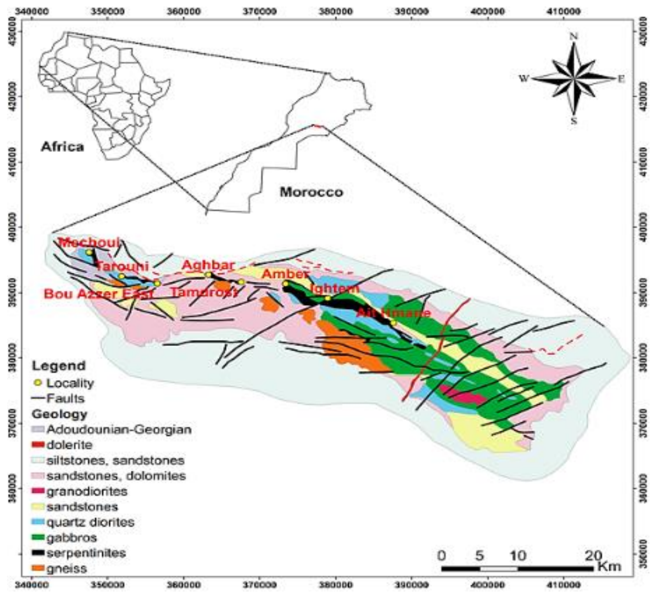

Figure 1. The geological map of the Bou Azzer inlier [20], [24]

The later non-metamorphic unit rests in a large unconformity on the Pan-African bedrock, its formations are composed at the base of sandstone levels, siltstones and rhyolites of the Lower Ediacaran age (NP3i) of the Tiddiline Group. All these lithostratigraphic units, from Cryogenian to Ediacaran, are straightened and folded into fault corridors at the late stage of the Pan-African tectonics. Subsequently, pyroclastic flows and volcano-detrital deposits of the Ouarzazate Group of the Upper Ediacaran age, composed mainly of ignimbrite pyroclastics from dacitic to rhyolite composition, occur in an angular unconformity with the Tiddiline Group.

2.2. Structural context

The Bou Azzer inlier is affected by several synschist, synmetamorphic (Eburnian and Pan-African) and late orogenic phases. The Pan-African orogeny is characterized by three tectonic phases. The first synschist ductile phase is responsible for orthogneissification, accompanied by shear structures with a predominantly dextral component [25]. The second phase B1 [20], [26] is characterized by a S1 schistose, synschistose anisoclinal folds of the main NW-SE direction and overlapping by descending chequered accidents [23]. On the other hand, the last late phase B2 [20] manifests itself in the form of folds that fill the B1 folds. These B2 folds, accompanied by fractured schistosity, have sub-horizontal direction axes from N100 to N140.

The Bou Azzer inlier then undergoes a second orogeny of Hercynian nature, responsible for the current structuring of the Anti-Atlas. This orogeny deforms the basement-cover complex with a sub-equatorial shortening of moderate intensity and decreasing from west to east [27].

3. Data and methodology

This study uses a remote sensing digital mapping approach to extract lineaments. By applying directional Sobel's filtering [28], [29], using four directions (N0°, N45°, N90° and N135°), a satellite image was obtained from Landsat 8 OLI on October 29, 2020 and freely downloaded from the European Space Agency website (https://glovis.usgs.gov) (Fig. 2).

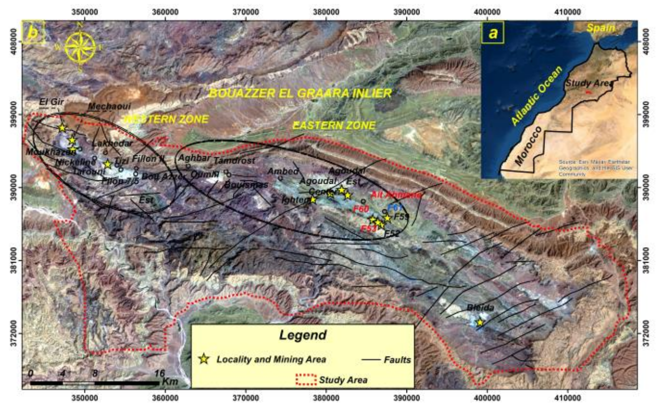

Figure 2. Location of the study area on the Landsat-8 Oli satellite image

Firstly, several steps of pre-processing and processing have been applied to the collected data using image processing software for lineament extraction, including radiometric calibration, atmospheric correction performed on the model (FLAASH) [30], [31].

Then, procedures have been conducted to improve the image quality of the data by applying Principal Component Analysis (PCA) [7]-[10], [32], [33].

Afterward, the lineament extraction was performed by applying different combinations of values for the LINE Module in the most commonly used Geomatica software [34]-[36]. Map verification has been obtained using a fracture map extracted from the geological map of the study area 1/50000 (Bou Azzer-El Graa), with their explanatory notes [13], [15], [16]. Thus, the work is complemented by field work, as well as a bibliographic synthesis. Finally, the prevailing tectonic regime and the regional stress field direction (σ1, σ2, σ3) have been determined. The main steps used for pre-processing and numerical data processing, as well as validation of the fracture map, are summarized in Figure 3.

4. Results and discussion

The results of the fracture density maps and the major directional rosettes presented in Figures 4, 5, 6 and 7, extracted from the new fracture map using a remote sensing methodological approach, show four systems of main orientations of the predominant major fractures in the study area: N0°, N45°, N90° and N135°.

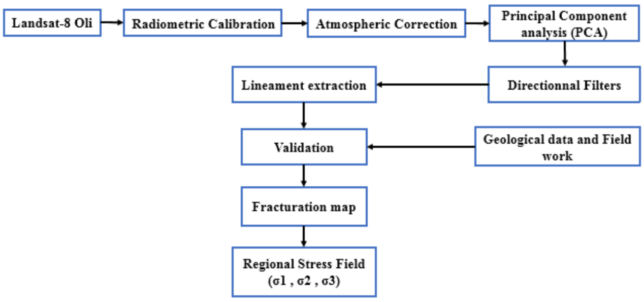

Figure 3. Methodological steps used in this study

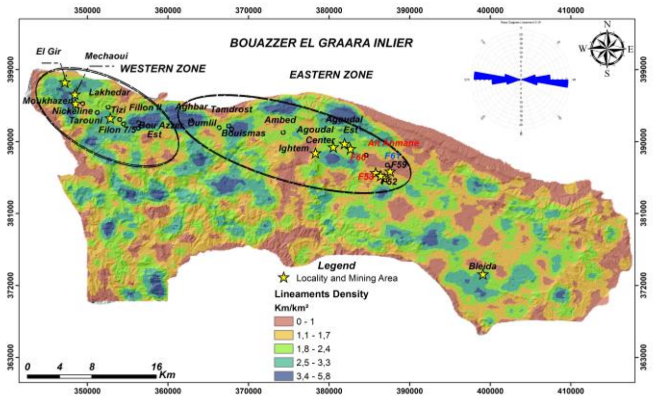

Figure 4. Results of the fracture density map and the major N90° directional rosette in the Bou Azzer inlier

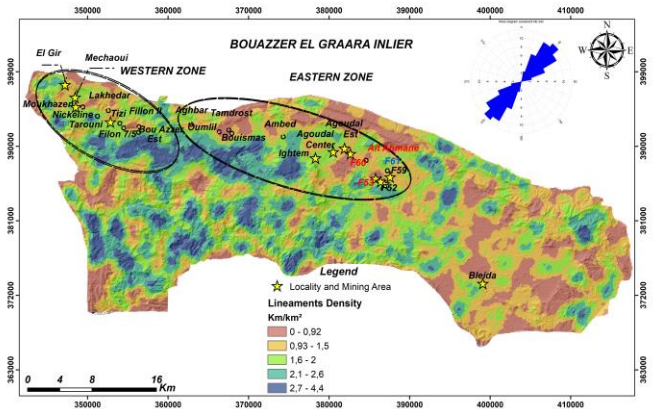

Figure 5. Results of mapping the fracture density and the major N45° directional rosette in the Bou Azzer inlier

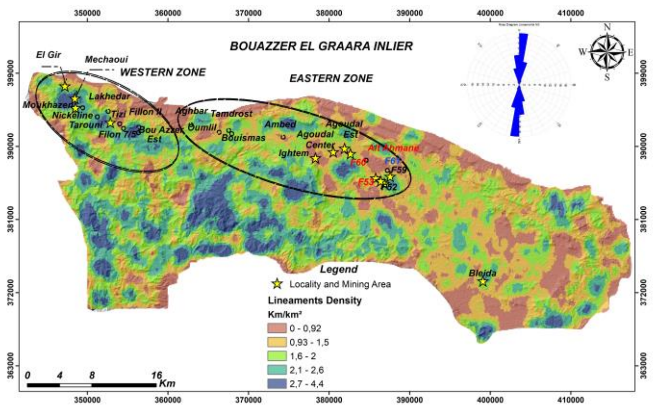

Figure 6. Results of mapping the fracture density and the major N0° directional rosette in the Bou Azzer inlier

The lineaments of the N90° direction are presented by a high density in the northwestern part and small areas in the central part of the study area.

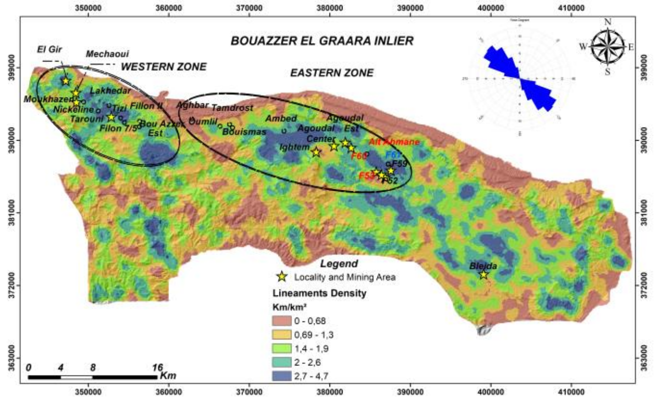

Figure 7. Results of mapping the fracture density and the major N135° directional rosette in the Bou Azzer inlier

The lineaments of the N45° direction are presented by a high density in the northwestern and southwestern parts of large areas.

The lineaments of the N0° direction are presented by a high density in the southwestern part of the Bou Azzer inlier.

The lineaments of the N135° direction are presented by a high density in the central part with distribution of small areas in the eastern and western parts of the Bou Azzer inlier.

A combination of structural analysis of the major mean directions in the Bou Azzer inlier and the bibliographic works according to [20], [37] makes it possible to identify several tectonic events of compressive constraints, the chronological sequence of which is as follows (Fig. 8).

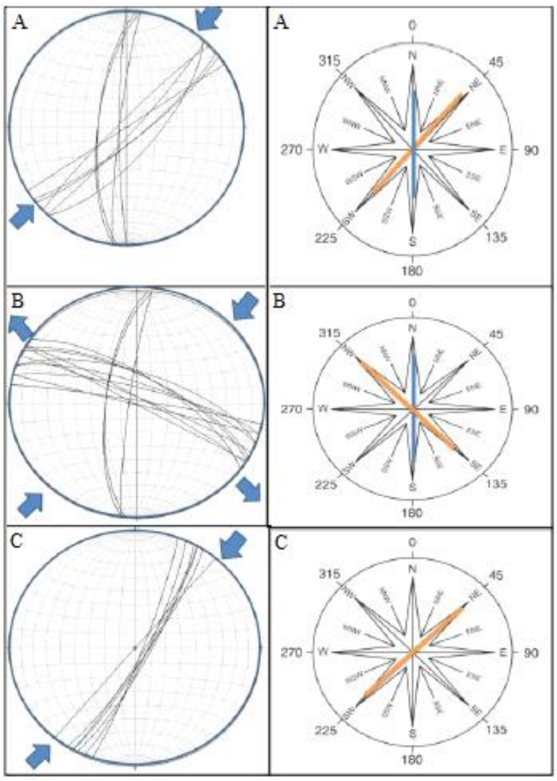

Figure 8. Stereographic representations of structures and determination of stress axes; (a) during N30 compression; (b) during ENE-WSW compression; (c) open quartz tension cracks during NE-SW compression

A tectonic episode with a compressive stress field is responsible for the reverse play of the N-S faults, a dextral strike-slip play of the NW-SE and NE-SW faults, as well as the sinistral strike-slip play of the ENE-WSW faults (Fig. 8a).

A tectonic episode is characterized by ENE-WSW oriented stress. This regime is responsible for the sinistral strike-slip play and several directional families of fractures without filling, but the most represented families are: E-W, N-S and NW-SE (Fig. 8b).

A tectonic episode, characterized by NNW-SSE oriented stress, is responsible for the sinistral strike-slip play of NE-SW faults and a dextral strike-slip play of WNW-ESE, as well as from NW-SE to NNW-SSE faults.

A tectonic episode is characterized by tension splits formed during a NE-SW trending compression episode (Fig. 8c). Most intra-serpentinite quartz veins show a sinistral play. The Pan-African deformation is highly heterogeneous, characterized by the presence of C/S shear planes organized into two families: N70-N100 sinistral and N140-N150 dextral.

The characterization of brittle and ductile structural elements to scale begins with in-situ surveys of fractures in the two sectors of Ait Ahmane and Ambed, located in the central part of the Bou Azzer inlier about forty kilometers southeast of the Bou Azzer mining center. Schistosity is one of the most striking structural elements of the relief, which gives the best idea of the tectonic stress direction, as it is the most represented plane in the rock. Two types of schistosity have been identified in the study area: S1 schistosity with orientation varying from N110° to N130° (Fig. 9a), and medium to strong dip between 60 and 85° southward.

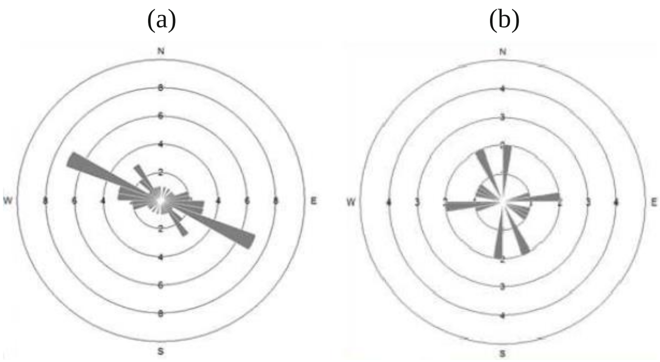

Figure 9. Stereograms: (a) stereogram of the S1 schistose planes; (b) stereogram of fractures filled with Ait Ahmane serpentinite

This S1 plane is mainly clogged with recrystallizations: carbonates, asbestos. The S1 schistosity is related to the Pan-African major phase [20]. The S2 schistosity varies from N130 to N160 with a dip varying from 55 to 75° to the southeast. This schistosity generally affects serpentinite and gabbros, as well as all the Cryogenian terrains (lower PII) of the Bou Azzer inlier (Fig. 10). The predominant fracture directions in the Ait Ahmane sector, as a rule, are two directions NW-SE and NNW-SSE with a dip varying from 60 to 85°, filled with quartz and carbonates. Thus, several families of directional fractures without filling are identified in the sector, but E-W, N-S and NW-SE families are most represented (Fig. 9b).

In the Ambed sector, brittle structures in the form of fractures with either quartz or quartz-carbonate filling belong to two families of NNW-SSE and N-S directions. Thus, NE-SW structures have a dip varying from 40 to 80°. Figure 11 shows fracturing in two facies: serpentinite and gabbro. Also in the Ambed area, in contacts of serpentinites with quartzite diorites and gabbros, veins filled quartz have been identified, ranging in size from a centimeter to a decimeter (Fig. 12).

Figure 10. Schistosity affects serpentinite and gabbros in the Bou Azzer inlier

Figure 11. Fracturing in the rock mass of serpentinite and gabbro

Figure 12. Quartz veins marking the contact between serpentinite and quartz diorite

These contacts tend to be faults that probably played out during the late brittle phases. Moreover, these quartz or quartz-carbonate veins and veinlets show sinistral displacements.

5. Conclusions

The study of fractures makes it possible to reconstruct the regional tectonic history both from the fracture kinematics and from the tectonic stress orientation. The regional stress field direction, determined in this work, can significantly improve the 2D, 3D geotechnical numerical models, as well as interpret deformations and displacements in the underground mining operations of the Bou Azzer mine.

These underground mining operations are subject to a heterogeneous tectonic stress field with a compressive tectonic regime. The direction of the principal stress $\sigma 1$ is N°30.

Acknowledgements

This research has been performed without any external funding.

References

[1] Hobbs, W.H. (1904). Lineaments of the Atlantic Border region. *Geological Society of America Bulletin*, *15*(1), 483-506. https://doi.org/10.1130/gsab-15-483

[2] Hashim, M., Ahmad, S., Johari, M.A.M., & Pour, A.B. (2013). Automatic lineament extraction in a heavily vegetated region using Landsat Enhanced Thematic Mapper (ETM+) imagery. *Advances in Space Research*, *51*(5), 874-890. https://doi.org/10.1016/j.asr.2012.10.004

[3] Hobbs, W.H. (1912). *Earth features and their meaning; an introduction to geology for the student and the general reader*. New York, United States: The Macmillan, 590 p. https://doi.org/10.5962/bhl.title.18732

[4] Marghany, M., & Hashim, M. (2010). Lineament mapping using multispectral remote sensing satellite data. *Research Journal of Applied Sciences*, *5*(2), 126-130. https://doi.org/10.3923/rjasci.2010.126.130

[5] Masoud, A., & Koike, K. (2006). Tectonic architecture through Landsat-7 ETM+/SRTM DEM-derived lineaments and relationship to the hydrogeologic setting in Siwa region, NW Egypt. *Journal of African Earth Sciences*, *45*(4-5), 467-477. https://doi.org/10.1016/j.jafrearsci.2006.04.005

[6] O'leary, D.W., Friedman, J.D., & Pohn, H.A. (1976). Lineament, linear, lineation: Some proposed new standards for old terms. *Geological Society of America Bulletin*, *87*(10), 1463. https://doi.org/10.1130/0016-7606(1976)87<1463:lllspn>2.0.co;2

[7] Massironi, M., Bertoldi, L., Calafa, P., Visonà, D., Bistacchi, A., Giardino, C., & Schiavo, A. (2008). Interpretation and processing of ASTER data for geological mapping and granitoids detection in the Saghro massif (eastern Anti-Atlas, Morocco). *Geosphere*, *4*(4), 736. https://doi.org/10.1130/ges00161.1

[8] El Janati, M., Soulaimani, A., Admou, H., Youbi, N., Hafid, A., & Hefferan, K.P. (2013). Application of ASTER remote sensing data to geological mapping of basement domains in arid regions: a case study from the Central Anti-Atlas, Iguerda inlier, Morocco. *Arabian Journal of Geosciences*, *7*(6), 2407-2422. https://doi.org/10.1007/s12517-013-0945-y

[9] Adiri, Z., El Harti, A., Maacha, A.J.L., & Bachaoui, E.M. (2016). Lithological mapping using Landsat 8 OLI and Terra ASTER multispectral data in the Bas Drâa inlier, Moroccan Anti Atlas. *Journal of Applied Remote Sensing*, *10*(1), 016005. https://doi.org/10.1117/1.jrs.10.016005

[10] Adiri, Z., El Harti, A., Jellouli, A., Lhissou, R., Maacha, L., Azmi, M., Zouhair, M., & Bachaoui, E.M. (2017). Comparison of Landsat-8, ASTER and Sentinel 1 satellite remote sensing data in automatic lineaments extraction: A case study of Sidi Flah-Bouskour inlier, Moroccan Anti Atlas. *Advances in Space Research*, *60*(11), 2355-2367. https://doi.org/10.1016/j.asr.2017.09.006

[11] El Janati, M. (2019). Application of remotely sensed ASTER data in detecting alteration hosting Cu, Ag and Au bearing mineralized zones in Taghdout area, Central Anti-Atlas of Morocco. *Journal of African Earth Sciences*, (151), 95-106. https://doi.org/10.1016/j.jafrearsci.2018.12.002

[12] Choubert, G. (1947). L'accident majeur de l'Anti-Atlas. *Comptes Rendus de l'Academie des Sciences*, (224), 1172-1173.

[13] Admou, H. (2011). Notice explicative, carte géol. Maroc (1/50000), feuille d'Aıt Ahmane. *Notes et Mémoires du Service Géologique*, (533), 1-7.

[14] Blein, O., Baudin, T., Chèvremont, P., Soulaimani, A., Admou, H., Gasquet, P., & Gombert, P. (2014). Geochronological constraints on the polycyclic magmatism in the Bou Azzer-El Graara inlier (Central Anti-Atlas Morocco). *Journal of African Earth Sciences*, (99), 287-306. https://doi.org/10.1016/j.jafrearsci.2014.04.021

[15] Chèvremont, P. (2013). ANZAR-Conseil, 2013. Notice explicative carte géological Maroc (1/50000), feuille Bou Azzer. *Notes et Mémoires du Service Géologique*, (535), 1-5.

[16] Souleimani, A. (2013). Notice explicative carte géologique Maroc (1/50000), feuille Al Glo'a. *Notes et Mémoires du Service Géologique*, (535), 13-15.

[17] Bodinier, J.L., Dupuy, C., & Dostal, J. (1984). Geochemistry of Precambrian ophiolites from Bou Azzer, Morocco. *Contributions to Mineralogy and Petrology*, *87*(1), 43-50. https://doi.org/10.1007/bf00371401

[18] Naidoo, D.D., Bloomer, S.H., Saquaque, A., & Hefferan, K. (1991). Geochemistry and significance of metavolcanic rocks from the Bou Azzer-El Graara ophiolite (Morocco). *Precambrian Research*, *53*(1-2), 79-97. https://doi.org/10.1016/0301-9268(91)90006-v

[19] El Hadi, H., & Tabit, H. (1989). Cumulats ultramafiques et mafiques du complexe ophiolitique de Bou Azzer El Graara (anti-atlas central, Maroc). *Publication Occasionnelle – Centre International Pour La Formation Et Les Échanges Géologiques*, (16), 1-12.

[20] Leblanc, M. (1975). *Ophiolites precambriennes et gites arsenies de cobalt : Bou Azzer (Maroc)*. These Doctorat d'Etat, Faculte des Science Paris VI, Memoires Centre Geologique et Geophysique.

[21] Leblanc, M., & Lancelot, J.R. (1980). Interprétation géodynamique du domaine pan-africain (Précambrien terminal) de l'Anti-Atlas (Maroc) à partir de données géologiques et géochronologiques. *Canadian Journal of Earth Sciences*, *17*(1), 142-155. https://doi.org/10.1139/e80-012

[22] Saquaque, A. (1992). *Un exemple de suture-arc: le Précambrien de l'Anti-Atlas centre oriental (Maroc)*. PhD Thesis.

[23] Saquaque, A., Admou, H., Karson, J., Hefferan, K., & Reuber, I. (1989). Precambrian accretionary tectonics in the Bou Azzer-El Graara region, Anti-Atlas, Morocco. *Geology*, *17*(12), 1107-1110. https://doi.org/10.1130/0091-7613(1989)017<1107:PATITB>2.3.CO;2

[24] Oberthür, T. (2009). Hercynian age of the cobalt-nickel-arsenide-(gold) ores, Bou Azzer, Anti-Atlas, Morocco: Re-Os, Sm-Nd, and U-Pb age determinations. *Economic Geology*, *104*(7), 1065-1079. https://doi.org/10.2113/econgeo.104.7.1065

[25] D'Lemos, R.S., Inglis, J.D., & Samson, S.D. (2006). A newly discovered orogenic event in Morocco: Neoproterozic ages for sup-posed Eburnean basement of the Bou Azzer inlier, Anti-Atlas Mountains. *Precambrian Research*, *147*(1), 65-78. https://doi.org/10.1016/j.precamres.2006.02.003

[26] Leblanc, M. (1981). The late proterozoic ophiolites of Bou Azzer (Morocco): Evidence for Pan-African plate tectonics. *Developments in Precambrian Geology*, (4), 435-451. https://doi.org/10.1016/S0166-2635(08)70022-7

[27] Soulaimani, A., Le Corre, C., & Farazdaq, R. (1997). Déformation hercyni-enne et relation socle/couverture dans le domaine du Bas-Draˆa (Anti-Atlas occidental, Maroc). *Journal of African Earth Sciences*, *24*(3), 271-284. https://doi.org/10.1016/S0899-5362(97)00043-2

[28] Alaoui, H.E., Moujahid, E., Ibouh, H., Bachnou, A., Babram, M.A., & Harti, A.E. (2016). Mapping and analysis of geological fractures extracted by re-mote sensing on Landsat TM images, example of the Imilchil-Tounfite area (Central High Atlas, Morocco). *Estudios Geologicos (Madrid)*, *72*(2), 12. https://doi.org/10.3989/egeol.42328.394

[29] Javhar, A., Chen, X., Bao, A., Jamshed, A., Yunus, M., Jovid, A., & Latipa, T. (2019). Comparison of multi-resolution optical landsat-8, sentinel-2 and radar sentinel-1 data for automatic lineament extraction: A case study of Alichur Area, SE Pamir. *Remote Sensing*, *11*(7), 778. https://doi.org/10.3390/rs11070778

[30] Gad, S., & Kusky, T. (2007). ASTER spectral ratioing for lithological mapping in the Arabian-Nubian shield, the Neoproterozoic Wadi Kid area, Sinai, Egypt. *Gondwana Research*, *11*(3), 326-335. https://doi.org/10.1016/j.gr.2006.02.010

[31] Pour, A.B., & Hashim, M. (2012). Identifying areas of high economic-potential copper mineralization using ASTER data in the Urumieh-Dokhtar Volcanic Belt, Iran. *Advances in Space Research*, *49*(4), 753-769. https://doi.org/10.1016/j.asr.2011.11.028

[32] Si Mhamdi, H., Raji, M., Maimouni, S., & Oukassou, M. (2017). Fractures network mapping using remote sensing in the Paleozoic massif of Tichka (Western High Atlas, Morocco). *Arabian Journal of Geosciences*, *10*(5), 125. https://doi.org/10.1007/s12517-017-2912-5

[33] Si Mhamdi, H., Raji, M., & Oukassou, M. (2016). Utilisation de la télédé-tection dans la cartographie automatique des linéaments géologiques du gran-itoïde de Tichka (Haut Atlas Occidental). *European Journal of Scientific Research*, (142), 321-333.

[34] Anbalagan, R., Kumar, R., Lakshmanan, K., Parida, S., & Neethu, S. (2015). Landslide hazard zonation mapping using frequency ratio and fuzzy logic approach, a case study of Lachung Valley, Sikkim. *Geoenvironmental Disasters*, *2*(1), 6. https://doi.org/10.1186/s40677-014-0009-y

[35] Mandal, S., & Maiti, R. (201). Role of lithological composition and lineaments in land sliding: A case study of Shivkhola watershed, Darjeeling Himalaya. *International Journal of Geology, Earth and Environmental Sciences*, (4), 126-132.

[36] Matori, A.N., Basith, A., & Harahap, I.S.H. (2011). Study of regional monsoonal effects on landslide hazard zonation in Cameron Highlands, Malaysia. *Arabian Journal of Geosciences*, *5*(5), 1069-1084. https://doi.org/10.1007/s12517-011-0309-4

[37] Hinaje, S. (1995). *Apport de l'analyse de la tectonique cassante tardi et post-panafricaine à la modélisation de la mise en place des minéralisations dans la boutonnière de Bou-azzer (anti-Atlas, Maroc).*

Визначення регіонального поля тектонічних напружень засобом дистанційного зондування у виступі Бу-Азер, центральна частина масиву Антіатлас, Марокко

А. Дріуч, Л. Уадіф, Х. Бенджмель, М. Бхіліссе, С. Ільмен

Мета. Визначення напрямку регіонального поля напружень виступу Бу-Азер за допомогою інструментів дистанційного зондування.

Методика. У цьому дослідженні використано підхід до цифрового картографування за допомогою дистанційного зондування, включаючи етапи попередньої та загальної обробки зображення з супутнику Landsat-8 OLI. Потім здійснено автоматичне вилучення лінеаментів на основі спрямованої фільтрації. Для визначення основних напрямків великих тектонічних тріщин ці результати були доповнені та підтверджені інтегрованою моделлю, яка включає синтез бібліографії та польових досліджень.

Результати. Результати аналізу спрямованої рози показують чотири системи основних напрямків, а саме N0°, N45°, N90° та N135°. Регіональне поле напружень на досліджуваній території, за даними історії тектоніки, характеризується тектонічним режимом горизонтального стиснення, про що вказують декілька систем зсувних розломів з високою тенденцією до деформації. Таким чином, велика кількість крихких і пластичних мікротектонічних показників підтверджує напрямок основного стискаючого напруження N°30. Напрямок тривимірного поля напружень: σ1: N°30, σ2: N°120, σ3: Вертикальна складова.

Наукова новизна. Проведене дослідження дає змогу визначити напрямок регіонального поля напружень виступу Бу-Азер, зокрема, на ділянках, уражених тектонікою різного масштабу складності, а також у важкодоступних ділянках.

Практична значимість. У гірничій практиці важливе значення має дослідження стійкості за допомогою 2D та 3D геотехнічного чисельного моделювання підземних гірничих виробок. Напрямок поля напружень є важливим вхідним параметром для розробки більш реалістичних моделей підтримки прийняття рішень, а також для забезпечення безпеки людей і матеріалів на шахті Бу-Азер.

Ключові слова: *Бу-Азер, дистанційне зондування, тріщина, інженерна геологія. поле напружень, моделювання*